

Instability threshold of a photorefractive pattern-forming system

Oliver Kamps,* Philip Jander, and Cornelia Denz

Institute of Applied Physics, Westfälische Wilhelms-Universität Münster, D-48149 Münster, Germany

(Received 11 January 2005; published 22 July 2005)

We report on the detailed experimental determination of the threshold for modulational instability in a photorefractive single-mirror feedback system using a Fourier control technique. Results are compared to analytical predictions and a disagreement for the experimentally significant multiple pattern region is found. Implications for the generation of nonhexagonal two-dimensional patterns are discussed.

DOI: [10.1103/PhysRevE.72.016215](https://doi.org/10.1103/PhysRevE.72.016215)

PACS number(s): 47.54.+r, 42.65.Sf, 42.65.Hw

I. INTRODUCTION

The spontaneous formation of two-dimensional periodic patterns out of a homogeneous initial state is a widely spread phenomenon in the natural sciences [1], observed in as diverse disciplines as chemistry, biology, hydrodynamics, solid-state physics, and nonlinear optics. A common feature of pattern forming systems is the existence of a control parameter threshold, where a homogeneous state becomes unstable against a periodic perturbation with a well defined wave number. Beyond this threshold, the perturbation grows and a periodic pattern arises. Due to their periodicity, the emerging structures can be characterized by only a few modes in Fourier space.

The connection between the instability of the homogeneous state and the control parameter can be obtained by means of a linear stability analysis. The result of this analysis is a threshold value for the control parameter in dependence on the wave number. Whereas the linear stability analysis is an often used tool to investigate a pattern forming system, the corresponding experimental determination of the instability thresholds is challenging. Whenever the homogeneous state is destabilized by increasing the control parameter in experiment, the pattern corresponding to the wave number with the lowest threshold grows. Therefore it is not possible to directly determine the thresholds for modulations with different wave numbers. However, this problem can be solved by confining the system response to a selectable wave number range. In this case the threshold value of any wave number can be determined by changing the control parameter until the homogeneous state changes into a periodic pattern with the selected wave number.

In optics, Fourier space is directly accessible through imaging using a single lens. With the help of a filter in Fourier space, it is possible to suppress all wave numbers except the one under consideration. Pesch *et al.* used this method for the first time to measure the marginal stability curve of a pattern forming optical system with sodium vapor as the nonlinear medium [2].

II. THEORETICAL DESCRIPTION

A. The single mirror feedback system

Spontaneous formation of hexagonal patterns in the photorefractive feedback system considered in this paper was first reported by Honda in 1993 [3]. The basic setup for investigating pattern formation in photorefractive media [4] is the single mirror feedback system (Fig. 1). The photorefractive medium is illuminated by a focused laser beam which, after passing it once, is reflected back by a mirror. The result of the interference of the two counterpropagating beams is a modulation of the refractive index of the medium due to the photorefractive effect. A periodically modulated index of refraction leads to the coupling of the energy and phases of the two beams. Above a certain threshold, two-beam coupling leads to a spontaneous transverse modulation of the beams and therefore to the generation of patterns.

In contrast to many other optical nonlinear pattern forming systems, the photorefractive medium is not a thin slice, but a bulk medium. Due to the nonlinear propagation of light in the bulk medium, additional nonlocal effects must be taken into account, which considerably complicate the theoretical treatment of this system. On the other hand, the considerable propagation within the nonlinear medium is a characteristic feature of the photorefractive medium, possibly responsible for the multitude of nonhexagonal patterns.

In one possible arrangement, the mirror is placed directly behind the crystal. However, we take advantage of an equivalent *virtual* mirror, created by two imaging lenses in the feedback path [5]. In this configuration, access to the Fourier plane of the feedback arm is available, which we will utilize for determination of the threshold curves. Additionally, negative feedback distances are accessible, where the

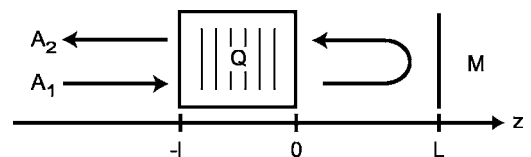


FIG. 1. Two wave-mixing configuration with a feedback mirror M . A_1 is the pump and A_2 is the reflected beam, Q is the refractive index grating amplitude, z indicates the direction of propagation. l is the medium length and L is the distance from the crystal face to the feedback mirror.

*Electronic address: okamp@uni-muenster.de

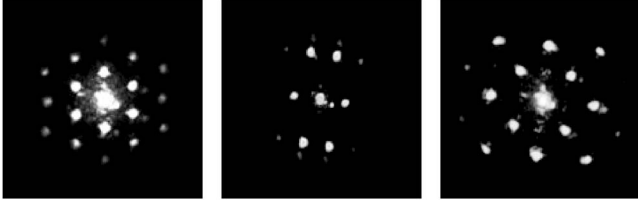


FIG. 2. Three example patterns observable in the photorefractive feedback system (Fourier space). The squeezed hexagon and the square pattern are found in the *multiple pattern region* whereas the hexagonal pattern is dominantly observed in the remaining parameter space.

virtual mirror plane is located inside of the crystal. The notion “inside” must be taken with caution in a nonlinear medium, as the medium beyond the mirror plane still affects the propagating waves. For mirror positions near the center of the crystal, different types of patterns like squares or hexagons are observed (Fig. 2). In this parameter range called *multiple pattern region* [5], multiple stable solutions are found to be available to the system for a single set of parameters. Honda *et al.* reported a disagreement between the transverse scale of the patterns predicted by the linear stability analysis and experimental data for the *multiple pattern region* [6]. From this point of view it is crucial to experimentally determine the marginal stability curves for this system.

B. Model equations

The model for photorefractive wave mixing through the formation of a reflection grating is based on the charge transport model of Kukharev *et al.* [7].

The single mirror feedback system is described by three differential equations [8,9]. The wave mixing process in the crystal is governed by the first two equations which are slowly varying envelope equations for the two lightfields A_1 and A_2 . In this case, z is the propagation coordinate scaled by the crystal length l , and Δ_\perp is the transverse Laplacian scaled by the beam waist w_0 ,

$$\begin{aligned} \partial_z A_1 + if\Delta_\perp A_1 &= -QA_2, \\ -\partial_z A_2 + if\Delta_\perp A_2 &= Q^* A_1, \\ \tau(I)\partial_t Q + Q &= \gamma \frac{A_1 A_2^*}{|A_1|^2 + |A_2|^2}. \end{aligned} \quad (1)$$

The third equation describes the temporal evolution of the complex amplitude of the reflection grating, where $\tau(I)$ is the intensity dependent relaxation time. The crucial assumption in (1) is that the time development of the beam envelopes is slaved to the grating amplitude, because of its slow evolution. The parameter γ is the photorefractive coupling constant which takes the role of the control parameter.

C. Linear stability analysis

The linear stability analysis was first performed by Honda and Banerjee [10] and extended by Schwab [11] for the case

of input beams with different frequencies. In this paper, we are only concerned with the case of degenerate beam frequencies. Starting from (1) for one transverse dimension ($k_\perp = k_x$) we introduce the ansatz

$$A_j(z, x) = A_j^0 [1 + A_j^+ \exp(ik_x x) + A_j^- \exp(-ik_x x)], \quad (2)$$

consisting of the plane wave solutions A_j^0 and a perturbation in the form of weak sidebands at a transverse wave number k_x . In order to guarantee a small perturbation we choose $A_j^+ \ll 1$ and $A_j^- \ll 1$. The incident beams have no sidebands and therefore we set

$$A_1^+(0) = A_2^-(0) = 0. \quad (3)$$

With the help of the boundary conditions

$$A_2^+(l) = \exp(-2ik_d l) A_1^+(l), \quad (4)$$

$$A_2^-(l) = \exp(-2ik_d l) A_1^-(l) \quad (5)$$

the feedback mirror is taken into account. Here l is the length of the photorefractive crystal, $k_d = k_x^2 / (2k_0 n_0)$ is the normalized transverse wave number and $d = n_0 L / l$ is the normalized position of the virtual mirror. L is the distance between the feedback mirror and the backface of the crystal (Fig. 1).

The linear stability analysis leads to a threshold condition of the form

$$\begin{aligned} \cos(wl)\cos(k_d l) + \frac{k_d l}{wl} \sin(wl)\sin(k_d l) + \frac{\gamma l}{2wl} \sin(wl)\cos[k_d l(1 \\ + 2d)] = 0 \end{aligned} \quad (6)$$

with $wl = \sqrt{(k_d l)^2 - (\frac{1}{2}\gamma l)^2}$. All parameters are chosen dimensionless to facilitate the comparison between theory and experiment.

The threshold condition (6) depends on the photorefractive coupling strength, the position of the virtual mirror and due to $k_d l$ on the transverse wave number k_x of the perturbation. For a given normalized mirror position d , Eq. (6) yields the critical threshold value of γl_c , where the homogeneous state becomes unstable against a perturbation with the wave number $k_d l$. For a fixed mirror distance d , the threshold condition reduces to the form $\gamma l (k_d l)|_{d=0}$. The evaluation of this formula leads to the curve of marginal stability for the chosen d , depicted in Fig. 3 for $d=0$.

The curve displays an absolute minimum followed by some local minima. In an experiment without Fourier filtering, the wave number corresponding to the absolute minimum appears. Because $\gamma l (k_d l)|_{d=0}$ depends on the mirror position, the wave numbers of the minima will change for different d . To illustrate this, the wave number of the absolute and the first local minimum are plotted against the mirror position in Fig. 4. The curves are symmetric with respect to the center of the crystal ($d=-0.5$).

III. EXPERIMENT

A. Experimental setup

The photorefractive single feedback system depicted in Fig. 5 consists of an iron-doped KNbO₃ crystal with a length

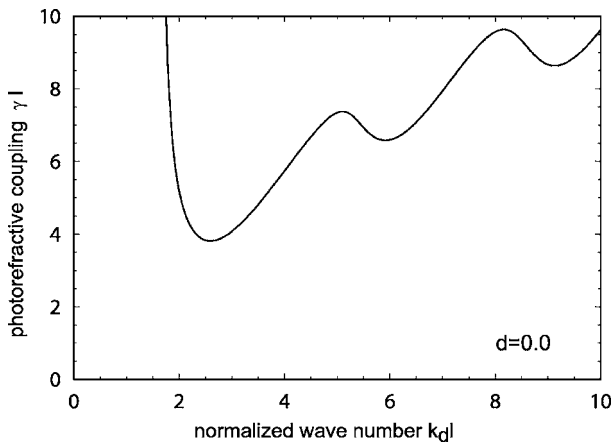


FIG. 3. Linear stability analysis, threshold curve for the virtual mirror located at the end of the crystal $d=0.0$.

of $l=5$ mm illuminated by a focused laser beam, and a feedback assembly with a moveable mirror (M2). A frequency doubled Nd:YAG laser operating at 532 nm cw with an output power of 100 mW is used as a coherent light source. Variable attenuation is provided by a half-wave plate and a polarizing beam splitter (p.BS). The optical diode (o.d.) prevents back reflection of light into the laser. The laser is focused into the crystal using a lens (L3) with a focal length of 450 mm with the resulting focus having about $300 \mu\text{m}$. An additional half-wave plate ($\lambda/2$) is used to adjust the polarization of the beam entering the crystal, which directly affects the photorefractive coupling strength γl by selection of the electrooptic coefficients. The crystal is tilted by about 5 degrees to avoid additional reflection at the crystal faces. The crystallographic c axis is oriented to provide amplification of the backpropagating beam. Instead of placing the feedback mirror directly behind the crystal, a $4f$ setup (L4 and L5) is used, which is completely equivalent to a feedback mirror positioned directly behind the crystal [11] and effectively creates a virtual mirror. Using the $4f$ imaging setup is convenient as it allows for virtual mirror positions

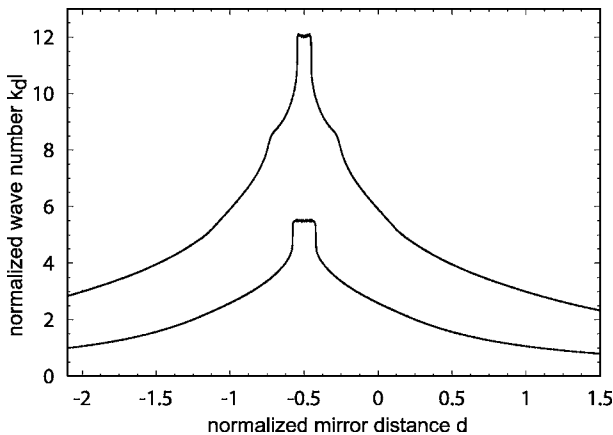


FIG. 4. Linear stability analysis, theoretical values for the minima of the threshold curves for varying values of the mirror position.

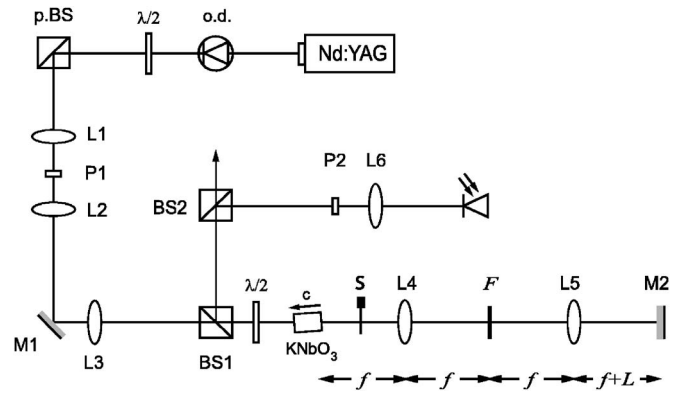


FIG. 5. Scheme of the experimental setup used to investigate pattern formation in the single mirror feedback configuration.

inside the KNbO_3 crystal and gives access to the Fourier plane \mathcal{F} where the Fourier filter can be placed.

B. The Fourier filter

The Fourier filter used to determine the marginal stability threshold needs to fulfill two tasks. On the one hand, it confines the system to one dimension by the slit mask depicted in Fig. 6(a). On the other hand, the wave number $k_{d,l_0}=0$ and the two symmetric sidebands with $+k_{d,l}$ and $-k_{d,l}$ must be able to pass the filter. To this end, the upper mask in Fig. 6(a) is combined with the lower one [Fig. 6(b)]. By laterally shifting the two masks against each other, only a small range of sidebands around a specific wave number is transmitted through the filter. The development of the intensity of the selected sidebands is observed by a photodiode (Fig. 5) as the control parameter is slowly increased. In the homogeneous system state only the wave number $k_{d,l_0}=0$ can be seen in the Fourier plane and only a low noise level is detected in the sideband photodiode. When the value of the control parameter is increased beyond the threshold for the chosen $k_{d,l}$, the power in all the sidebands will grow. Repeating this procedure for all available wave numbers, we can determine the complete threshold curves for the onset of modulational instability.

C. Experimental results

Two examples of the experimentally obtained thresholds in dependence on the normalized transverse wave numbers

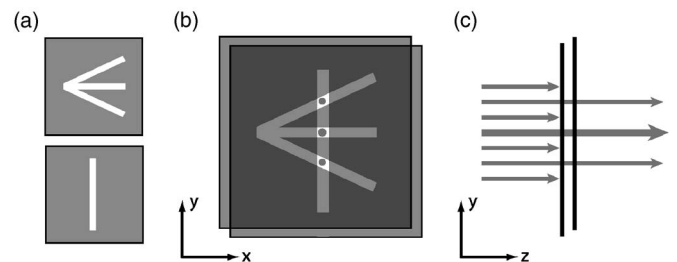


FIG. 6. (a) The two components of the Fourier filter, (b) arrangement of the two masks in the experiment, (c) view from a direction perpendicular to the z axis, illustrating that all but a selected band of wave numbers are blocked by the filter.

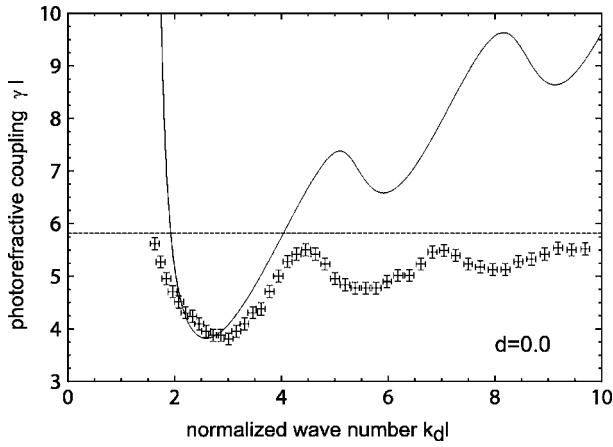


FIG. 7. Experimental threshold data superimposed on analytical prediction. Mirror position at the back face of the crystal (outside of multiple pattern region). Wave numbers of minima agree reasonably well, the actual coupling strength values do not fit.

are depicted in Figs. 7 and 8. The horizontal line marks the highest photorefractive coupling strength (γl) provided by the crystal used in the experiments.

For mirror positions outside of the medium, the absolute minima of the experimentally obtained γl values are in agreement with the theory (not shown). Due to the fact that the absolute value of γl_0 cannot be determined exactly, the absolute minimum of the numerical data is used to calibrate the experimental data given in this paper, in order to facilitate comparison of the marginal stability curves. However, the absolute value of the photorefractive coupling strength is without significance to the work presented in this paper. Only relative values of γl and the wave numbers of the minima are relevant.

At the mirror position $d=0$ (Fig. 7) the sequence of the minima is in agreement with the theory. But when the mirror is moved into the crystal, the situation changes. At $d=-0.63$ (Fig. 8) there is a significant difference between the shape of the curve formed by the measured points and the threshold curve.

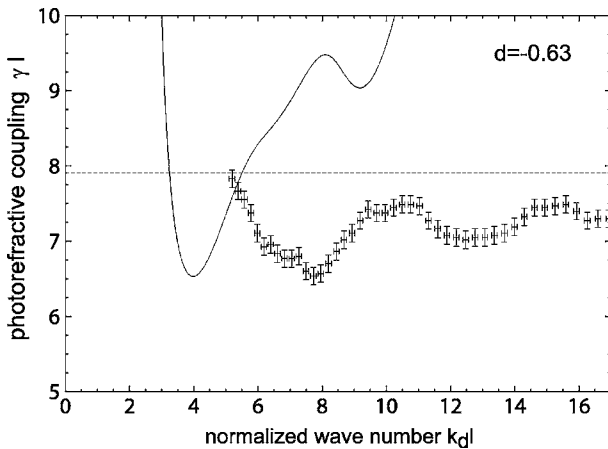


FIG. 8. Experimental threshold data superimposed on analytical prediction. Mirror position within the front third of the crystal (within the multiple pattern region). No quantitative agreement exists.

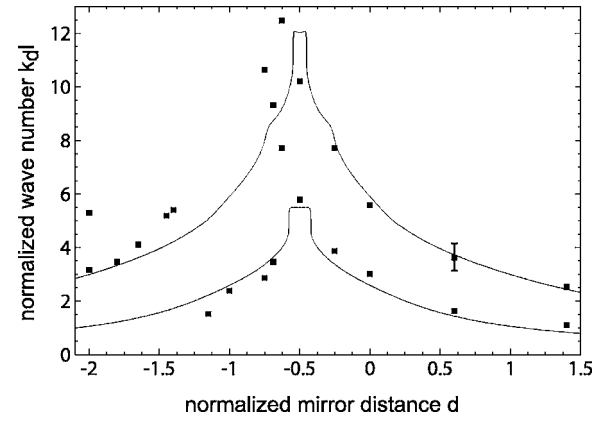


FIG. 9. Wave numbers of the threshold minima, analytical and experimental data. The precision of the mirror position is better than ± 0.005 ($\approx 10 \mu\text{m}$). A disagreement between both data sets is found for mirror positions mainly within the crystal ($-1.5 < d < 0$).

To clarify the influence of the virtual mirror position, the first two wave number minima of the thresholds are plotted against the mirror position d (Fig. 9). The black squares denote the measured values whereas the lines are the theoretical curves repeated from Fig. 4. It is remarkable, that in experiment the symmetry of the curves in respect to the center of the crystal is broken. While the analytical threshold decreases from the crystal center towards the backface, the measured values increase. Wave numbers larger than $k_d l = 13$ were not accessible in the experiment. The measured values near the lower curve for $d \geq -0.6$ belong to a minimum that appears in this parameter region.

With growing distance from the crystal, the experimental data approach the theoretical curves. In these regions, the observed patterns and pattern sizes match the predictions from the linear stability analysis.

D. Transverse size of patterns

As the actual pattern forming system features two transverse dimensions, we now compare the marginal stability curves measured under one-dimensional feedback with wave numbers observed in unconfined patterns. Both are related, as the modes with the lowest threshold values are expected to be dominant above threshold too, due to their initial strong growth (winner-takes-it-all dynamics).

In order to confirm this relation, we first investigate the dependence of the dominant mode's wave number on the coupling strength. Figure 10(a) repeats the threshold around the absolute minimum at mirror position $d=0$. Figure 10(b) exemplarily shows the rise time for modes with corresponding wave numbers at the maximum coupling strength. The fastest growing and hence dominant mode above threshold closely corresponds to the mode with the lowest threshold value. Thus a comparison of the wave numbers of two-dimensional patterns with the experimental threshold curves is valid and we expect a close relation.

Figure 11 displays wave number data for two-dimensional patterns on which experimental data from Fig. 9 is superimposed from two different crystal samples with no fitting em-

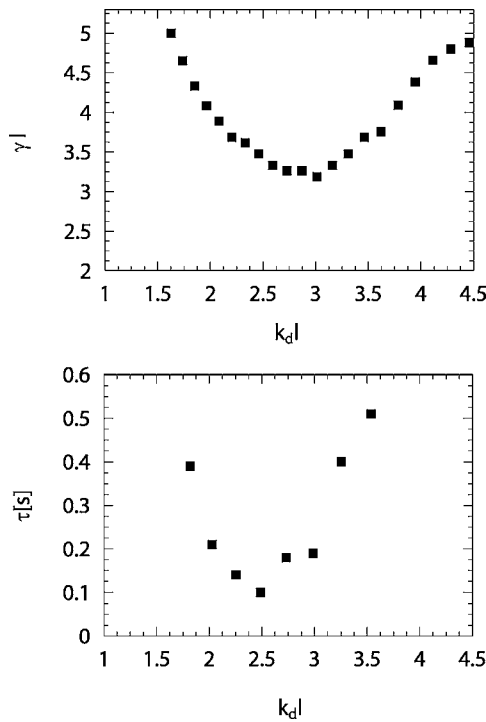


FIG. 10. Comparison of mode thresholds and mode growth rates above threshold. Top, threshold coupling strength values for different wave numbers. Bottom, rise time for modes with different wave numbers. The lowest threshold wave number band is found to be strongly growing above threshold. All data is given for mirror position $d=0$.

ployed. Each dot represents a wave number of a pattern constituent in the unconfined system. The pattern data display the asymmetry already reported by Honda *et al.* [6] and the strong correlation with the position of the minima of the experimental marginal stability curves (squares) indicates that the generation of patterns is in fact related to the threshold minima and that both differ from analytical predictions in the same manner. For several pattern constituents, no corresponding threshold minimum has been found, these wave

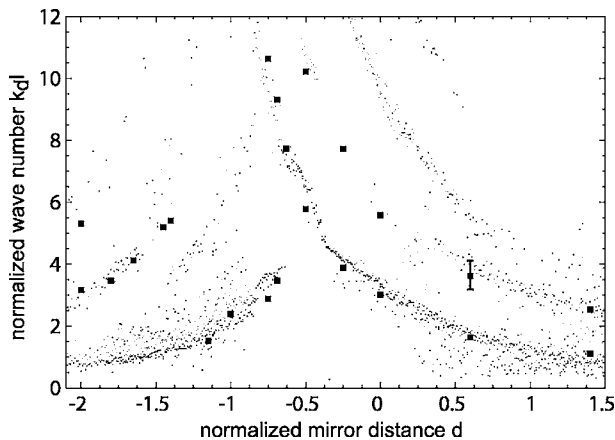


FIG. 11. Wave numbers of two-dimensional patterns (dots) compared with threshold minima in the one-dimensional threshold determination. A strong correlation between both sets of data is found.

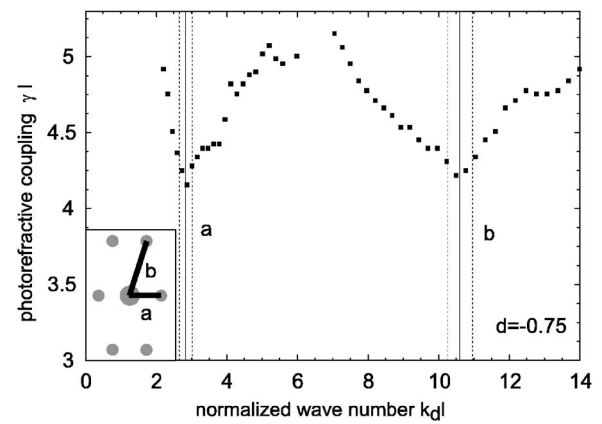


FIG. 12. Threshold curves at a mirror position where the squeezed hexagonal pattern is observed. The wave numbers of this pattern are marked and directly correspond to the threshold minima explaining the generation of a thin nonhexagonal pattern.

numbers may result from two-dimensional interaction of the active modes' wave vectors. However, the existence of a specific class of patterns can be traced directly to the interaction of independent modes, as we will show in the next section.

E. Implications for nonhexagonal patterns

Over most of the available parameter space, a single absolute minimum threshold exists (e.g., Fig. 7) and hexagonal patterns incorporating only the wave number corresponding to that minimum are observed. Usually, the dominance and stability of hexagonal patterns is explained in terms of a resonant excitation between three modes with the fundamental wave number [12]. However, in one part of the multiple pattern region (about $d=-0.75$), two equal minima are found (Fig. 12). At this mirror location, the squeezed hexagonal pattern (Fig. 2 center) is predominant. This pattern is composed of three wave vectors with two wave numbers, which coincide with the wave numbers of the threshold minima. Just as with normal hexagons, this pattern has a geometrical arrangement of three wave vectors where a resonant excitation of all three wave vectors is possible. Therefore, the existence of two equal threshold minima should be considered responsible for the generation of this nonhexagonal pattern which was to our knowledge unexplained up to now.

IV. CONCLUSION

We presented a detailed experimental analysis of the modulational instability threshold in a single mirror feedback system using a photorefractive nonlinearity. A Fourier control method was used to restrict the system to small bands of transverse wave numbers and the threshold for the spontaneous growth of a modulation was measured subsequently, scanning the available parameter range. We compared the results with analytical predictions obtained by means of a linear stability analysis and found a disagreement for virtual

mirror positions within the crystal, but otherwise good agreement. The wave number of minimum threshold values are shown to directly correspond to wave numbers of pattern constituents. Considering a specific nonhexagonal pattern, we find cooperation of independent modes to be responsible for its generation, connecting the observed disagreement between theory and experiment with the existence of nonhexagonal patterns in the multiple pattern region parameter

range. The reason for the observed inconsistency between analytical and experimental threshold is unknown at the time of writing and subject of ongoing research.

ACKNOWLEDGMENT

The authors acknowledge support by the Deutsche Forschungsgemeinschaft under Grant No. DE-486/10.

-
- [1] M. C. Cross and P. C. Hohenberg, *Rev. Mod. Phys.* **65**, 851 (1993).
- [2] M. Pesch, E. Große Westhoff, T. Ackemann, and W. Lange, *Phys. Rev. E* **68**, 016209 (2003).
- [3] T. Honda, *Opt. Lett.* **18**, 598 (1993).
- [4] C. Denz, Ph. Jander, M. Schwab, O. Sandfuchs, M. R. Belić, and F. Kaiser, *Ann. Phys. (N.Y.)* **13**, 391 (2004).
- [5] M. Schwab, C. Denz, and M. Saffman, *Appl. Phys. B: Lasers Opt.* **69**, 429 (1999).
- [6] T. Honda, H. Matsumoto, M. Sedlatschek, C. Denz, and T. Tschudi, *Opt. Commun.* **133**, 293 (1997).
- [7] N. V. Kukhtarev, V. B. Markov, S. G. Odoulov, M. S. Soskin, and V. L. Vinetskii, *Ferroelectrics* **22**, 949 (1979).
- [8] O. Sandfuchs, F. Kaiser, and M. R. Belić, *Phys. Rev. A* **64**, 063809 (2001).
- [9] O. Sandfuchs, *Self-Organization, Amplitude Equations and Fourier Control in a Nonlinear Optical Feedback System* (Shaker Verlag, Aachen, 2001).
- [10] T. Honda and P. Banerjee, *Opt. Lett.* **21**, 778 (1996).
- [11] C. Denz, M. Schwab, and C. Weilnau, *Transverse Pattern Formation in Photorefractive Optics* (Springer-Verlag, Heidelberg, 2003).
- [12] P. M. Lushnikov, *J. Exp. Theor. Phys.* **86**, 614 (1998).